IJST (2012) A2: 189-211
Iranian Journal of Science & Technology

http://www.shirazu.ac.ir/en

Sturctural flexibility under oxidative coupling of methane; main chemical role of alkali ion in [Mn+(Li, Na, K or Cs)+W]/SiO_2 catalysts

Z. Gholipour[1], A. Malekzadeh[1]*, M. Ghiasi[1], Y. Mortazavi[2] and A. Khodadadi[2]

[1]*School of Chemistry, Damghan University (DU), Damghan, Iran*
[2]*School of Chemical Engineering, University of Tehran, Tehran, Iran*
E-mails: malekzadeh@du.ac.ir, azim.malekzadeh@gmail.com

Abstract

Oxidative coupling of methane has been studied over (Mn+A+W)/SiO_2 catalysts in a continuous–flow micro reactor, where A represents an alkali ion of Li, Na, K or Cs having different weight percents. The main aim of this study is to find the role of alkali ions in interaction between Mn and W species with SiO_2 to make a proper structure for catalyzing oxidative coupling of methane (OCM) reaction. The catalysts were characterized by XRD, SEM, FTIR, TPR and also the electrical conductivity was measured in air and under OCM reaction. It was found that for the formation of crystallized catalyst, the amount of alkali ion should be such that the catalyst containing tungsten transforms into A_2WO_4. Using a smaller amount of alkali ions does not result in crystalline catalyst by calcination under the same condition of temperature and atmosphere. However, under the OCM reaction condition the catalyst gradually turns into a crystalline structure and its catalytic performance, i.e. conversion and selectivity, for the OCM reaction is almost similar to the (Mn+A_2WO_4)/SiO_2 catalyst. The transformation of the catalyst containing alkali ions from amorphous to crystalline one indicates a kind of structural flexibility of the catalyst under OCM atmosphere. The structural flexibility of the catalyst under the OCM reaction is considered to be the main chemical role of the alkali ions.

Keywords: Oxidative coupling of methane (OCM); manganes oxide; alkali ion; electrical conductivity; TPR

1. Introduction

Ethylene, the lightest alkene, is among the most produced organic compounds in the world. It is known as a base chemical in petrochemical industries and has a large market all over the world [1]. An increasing demand for ethylene both in developed and developing countries caused the annual production of ethylene to exceed 75 million metric tonnes in 2005 [2]. Accordingly, very large complexes for ethylene production are being built globally.

The natural gas, which is finding a more important role in energy and industry, has no contribution in ethylene production. The most famous established technology for natural gas conversion is steam reforming for production of synthesis gas [3]. However, continuous direct conversion of methane to olefins, methanol or formaldehyde is among the hottest researches in C_1 chemistry [4-5].

Among the continuous direct conversions of methane to higher value added products, the most noteworthy is the direct catalytic conversion of methane to C_2 hydrocarbons by OCM. During the past decades an attempt has been made to improve different aspects of catalytic OCM reaction including the catalysts [5-22]. Among the large number of catalyst systems which have been introduced, the (Mn+Na_2WO_4)/SiO_2 sample, first reported by Li and his co–workers, has attracted great attention because of its excellent catalytic performance and stability [7-23]. Experimental results under different conditions and the stability tests suggest that the (Mn+Na_2WO_4)/SiO_2 catalyst has alluring prospects in commercial applications [14-15].

The role of different components and the nature of the active centers of trimetallic (Mn+Na+W)/SiO_2 catalyst in the OCM reaction is very complicated [9-12]. Phase transition from amorphous silica to α-cristobalite was reported as a crucially important requirement for generating an active and a highly selective OCM catalyst [7, 9-12]. Favorable phase transition of amorphous silica to highly crystalline α-cristobalite was observed to take place in presence of small amounts of an alkali

*Corresponding author
Received: 1 November 2010 / Accepted: 18 February 2012

ion as a mineralizing agent [7, 9-10]. Sodium was also reported to increase the surface basicity as a requirement for high C_2 selectivity [8].

Manganese oxides were proposed to provide a more facile path for electron transfer to the oxygen adsorbed on the catalyst surface, thereby increasing the catalyst activity, especially at low temperatures [11-12]. Synergetic effect of two essential components i.e., metal oxide and sodium tungstate, was considered as a parameter for selective oxidation of methane over (Mn+Na+W)/SiO_2 catalysts [9]. Tungsten ions were proposed to stabilize the catalyst [8].

Surface WO_4^{2-} tetrahedron was reported as the site that is required for the OCM reaction over [Mn+(Li, Na or K)+W]/SiO_2 catalysts [16, 18]. Spillover of the oxygen, activated over manganese oxide, was reported to take place at tetrahedral WO_4^{2-} surface species, having one W=O and three W-O-Si surface bonds as the OCM active sites [16-17]. The WO_4^{2-} appears to have a strong interaction with support in the form of α-cristobalite, stabilized in the [Mn+(Na or K)+W]/SiO_2 catalysts [16, 20]. Weak interaction, however, is observed between WO_4^{2-} and support in the form of amorphous (Mn+W)/SiO_2 or quartz (Mn+Li+W)/SiO_2 catalysts [16].

A more facile generation of a transition state for methane activation was considered to form by the tetrahedral tungsten ions rather than that of the octahedral one in the (Mn+Na+W)/SiO_2 catalyst [16]. It was noted that tetrahedral tungsten ions have potential importance in achieving high CH_4 conversion and C_2 selectivity in the (Mn+Na+W)/SiO_2 catalysts [16]. The formation of the tetrahedral tungsten ions was shown to critically depend on the presence of sodium ion [16]. A rapid drop of a high initial CH_4 conversion and C_2 selectivity in the (Mn+Li+W)/SiO_2 catalyst was attributed to a decrease in the tetrahedral tungsten ions [16]. The role of alkali ion and crystal structure in the formation of an active and selective catalyst, however, is still open for study. In this research we have investigated the role of alkali ion in the catalytic system of (Mn+W)/SiO_2, containing different amounts of alkali ions of Li, Na, K or Cs. The focus is on the chemical role of alkali ions.

2. Experimental

Catalysts containing 4.0 wt% Mn, 3.1 wt% W and different loadings of alkali ions of Li, Na, K or Cs, were prepared by incipient wetness of the amorphous silica support (60–100 mesh size silica gel, Davisil grade 645 from Aldrich) with solution of the precursors [19-20]. The weight percents of manganese and tungsten were selected according to the metal loading in trimetallic (4.0 wt% Mn + 5.0 wt% Na_2WO_4)/SiO_2 catalyst. The (4.0 wt% Mn + 5.0 wt% A_2WO_4)/SiO_2 catalysts, in which A is an alkali ion, were also prepared by similar method. Manganese and alkali ion impregnation were performed using an aqueous solution of the metal nitrates with appropriate concentrations. Tungsten impregnation was performed by using an aqueous solution of tungsten with proper concentration. The SiO_2 impregnated with manganese nitrate was dried at 150°C overnight, followed by impregnating with alkali ions and tungsten solution. The prepared catalysts were then dried at 150°C overnight, followed by calcining at different temperatures for 8 h.

X–ray diffraction patterns of the freshly calcined and used catalysts were recorded in a Bruker AXS diffractometer D8 ADVANCE with Cu–Kα radiation filtered by a nickel monochromator and operated at 40 KV and 30 mA. Diffraction patterns were recorded in the range of $2\theta = 10–70^o$.

The IR spectra of the catalysts were recorded by mixing an appropriate amount of each sample with potassium bromide in a PERKIN–ELMER FTIR spectrometer. The diluted samples were pelletized into 13 mm diameter thin pellets. Each pellet was then placed in a holder plate and located vertically into the FTIR unit. The infra–red spectra were obtained over a wave number range of the 400–1600 cm^{-1}.

Temperature programmed reduction of the catalysts was performed using a CHEMBET 3000 from Quanta Chrome Corporation. A flow rate of 10 mL/min of 2.7% H_2 in nitrogen gas stream was used through a quartz U tube containing 50 mg of the catalyst. Hydrogen consumption was analyzed using a TCD detector. The data were logged into an online computer for analysis.

Scanning electron microscopic (SEM) studies were carried out using a scanning microscope of Philips Company. The samples were prepared by the gold ion sputtering technique.

The direct current electric conductivity of various catalysts was measured using an electric conductivity measurement set–up equipped with a home–made quartz cell in which 500 mg of catalyst was placed between the two 24 K gold electrodes on quartz wool [23]. The electric conductivity measurements were carried out in oxidizing atmosphere of air or oxygen and also during the OCM reaction at 800°C. The reported electrical conductivity (σ) is the value that is measured under isothermal steady state conditions and is the reciprocal of the catalyst resistance, R_{cat}, calculated using a method reported elsewhere [23].

The electrical conductivity measurements and the catalytic performance of different catalysts for the

OCM reaction were performed at 800°C in a quartz reactor [23]. A mixture of CH_4/air =1 or CH_4/O_2 =5, containing 115 mL/min (STP), was passed over 500 mg of the catalyst bed supported on some quartz wool. The reaction products were analyzed by a gas chromatograph (GC) having a FI detector equiped with a methanizer. The blank run in the absence of catalyst resulted in less than 1% methane conversion and no appreciable conductance.

3. Results and discussion

Crystallization of amorphous silica to highly crystalline phases takes place during the calcination of samples at 775–850°C in the presence of an alkali ion, especially in the form of alkali tungstate [7, 9-11, 13-23]. The representative XRD patterns of the fresh and spent (4%Mn+*x*%A+3.13W)/SiO_2 and (4%Mn+5%A_2WO_4)/SiO_2 catalysts are shown in Figs. 1-3. Here A is an alkali ion of Li, Na, K or Cs and *x* is 0.1 or 0.78. The crystallinity percent of different catalysts is shown in Table 1 [23]. The crystalline (Mn+Na_2WO_4)/SiO_2 and (Mn+Li_2WO_4)/SiO_2 samples are considered as reference to calculate the crystallinity percent of different catalysts.

The crystalline phases of the fresh and spent catalysts containing different alkali ions, reported in the literature, are shown in Tables 2-3. Quartz is determined to be the main crystalline phase of the catalysts containing Li ion. The α–cristobalite, however, is determined as the main crystalline phase of catalysts containing Na, K or Cs ion. New crystalline phases appear by the change in loading of different components of Mn, W or alkali ions. The data of this work, determined according to the analysis of XRD patterns of Figs. 1-3, are shown in Table 4. The XRD patterns analyses were carried out according to the library of the XRD instruments. Figures 1-3 and Tables 1 and 4 show that the crystalline structure and crystallinity percent of the catalysts depend on the loading of alkali ion and the conditions of calcination or reaction. The crystalline phases of tridymite, crystoballite, quartz and silicon dioxide are observed in the catalysts containing different loading of the alkali ions. The main crystalline phase of the fresh (Mn+0.1wt%Li+W)/SiO_2 catalyst is determined to be cristobalite (Fig. 1 and Table 4). The (Mn+0.1wt%Li+W)/SiO_2 catalyst, however, turns into the quartz as the main crystalline form after 12 h under OCM reaction condition. The main crystalline phase of the catalysts containing 0.27 wt% and 0.78 wt% Li ion is determined to be quartz for the fresh catalyst and for the one exposed to the OCM reaction for 12 h. The quartz is accordingly determined as the final crystalline structure of [Mn + (0.1, 0.27 or 0.78)wt%Li + W)]/SiO_2 catalysts [9-10, 16, 19]. Quartz was determined as the main crystalline phase of (Mn+Na_2WO_4)/SiO_2 catalysts after 1000 h on OCM reaction conditions (Table 2) [15]. Increase in Li ion loading to 0.78wt% is observed to accompany the appearance of a new crystalline phase of $Li_2Si_2O_5$ in the spent (Mn+0.78%Li+W)/SiO_2 catalyst (Figure 1 and Table 4).

Similar results are observed for the catalysts containing different amounts of Na, K or Cs ions (Figs. 2-3 and Table 4). Low crystallinity is observed for the fresh [Mn+0.1wt%(Na, K or Cs)+W)/SiO_2 and (Mn+0.78wt%Cs+W)/SiO_2 catalysts (Fig. 2 and Table 1). The crystallinity, however, is observed to increase after 12 h on OCM reaction (Figs. 2-3 and Table 1). Cristobalite is determined to be the main crystalline phase of catalysts containing Na, K or Cs ion (Figs. 2-3 and Table 4). The quartz crystalline phase, however, is surprisingly observed as much as the crystoballite crystalline form in the spent catalyst (Mn+0.1wt% Na+W)/SiO_2 after 12 h on OCM reaction (Fig. 3 and Table 4). Presence of the cristobalite and quartz crystalline forms in the fresh catalyst containing 0.1wt% Li and the spent ones containing 0.1wt% Na, K or Cs indicate a complicated transformation of the amorphous silica to the crystallized form. This transformation is very slow and requires heating at 1600°C for a long period of time [19]. However, it is facilitated in the presence of small amounts of an alkali ion and alkali tungstate as mineralizing agents. Manganese oxides and/or tungstate alone cannot induce silica phase transition. The mechanism of this process is not clear. However, it is well documented that the basic chemistry underlying this drastic variation in silica phase transition behavior is the breaking of the Si-O bond of the pure silica by alkali ion and the concomitant appearance of the so-called non-bridging oxygen, which is linked on one side to silicon and on the other side to the alkali ion [19]. XRD patterns of the fresh [Mn+(0.1 or 0.78) wt%Cs+W]/SiO_2 catalysts, calcined for 8 h at 900°C, and the spent (Mn+0.1wt%Cs+W)/SiO_2 catalyst show that the crystallization of the catalysts during OCM reaction is not due to the temperature rising under the reaction condition (Fig. 4).

Amorphous feature, observed for the low amount of Na, K and Cs ion containing catalysts, shows that the crystallization that takes place by the alkali ion critically depends on the alkali ion loading in the catalyst and the condition of calcination. Moles of alkali ion required for the formation of alkali tungstate provide the best conditions for crystallization during the calcination at air atmosphere. In addition, it is observed that the alkali ion loading in the catalyst is much more important than the type of alkali ion for obtaining a fully crystallized catalyst. The crystalline phase of catalyst to be tridymite, cristobalite or quartz, however, is observed to depend on loading of the alkali ion.

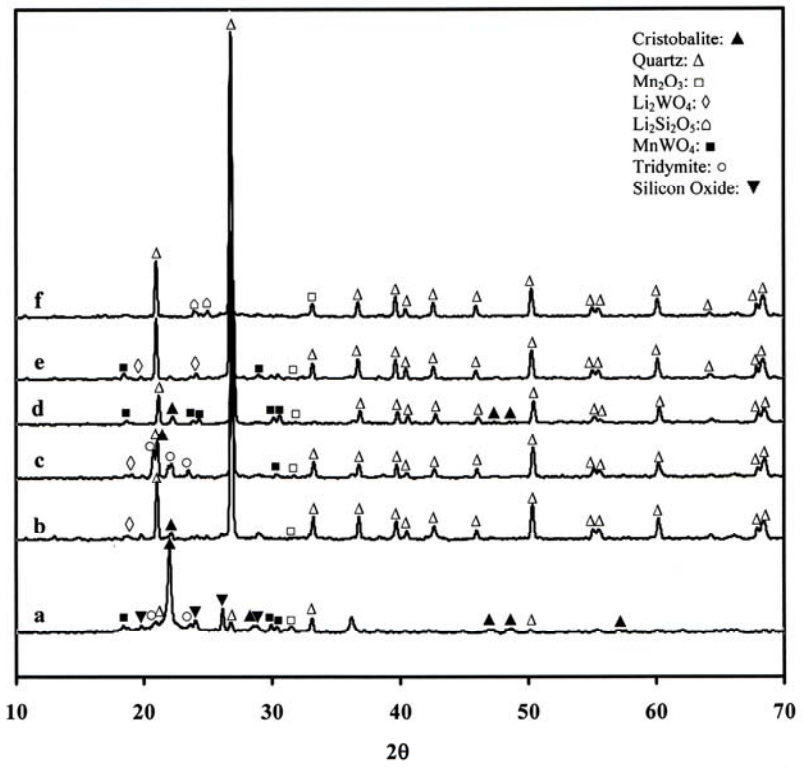

Fig. 1. XRD patterns of fresh (Mn+0.1%Li+W)/SiO_2 (a), (Mn+5%Li_2WO_4)/SiO_2 (b) and (Mn+0.78%Li+W)/SiO_2 (c) catalysts after 8 h calcination at 800°C. d, e and f are for spent catalysts after 12 h on OCM reaction conditions, respectively

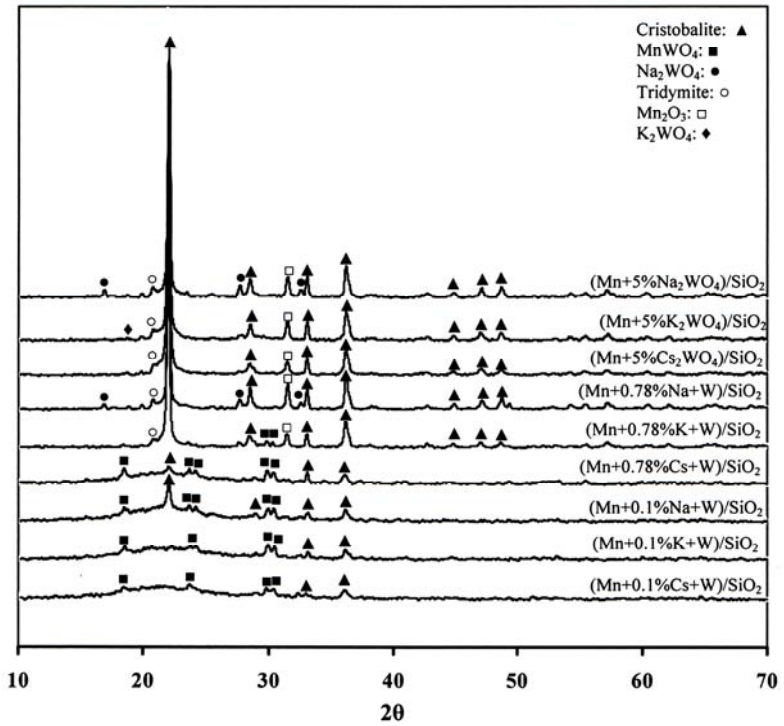

Fig. 2. XRD patterns of fresh [4wt%Mn+(0.1 or 0.78)wt%(Na, K or Cs)+3.13wt% W]/SiO_2 and [4wt%Mn+5wt%(Na, K or $Cs)_2WO_4$]/SiO_2 catalysts after 8h calcining at 800°C

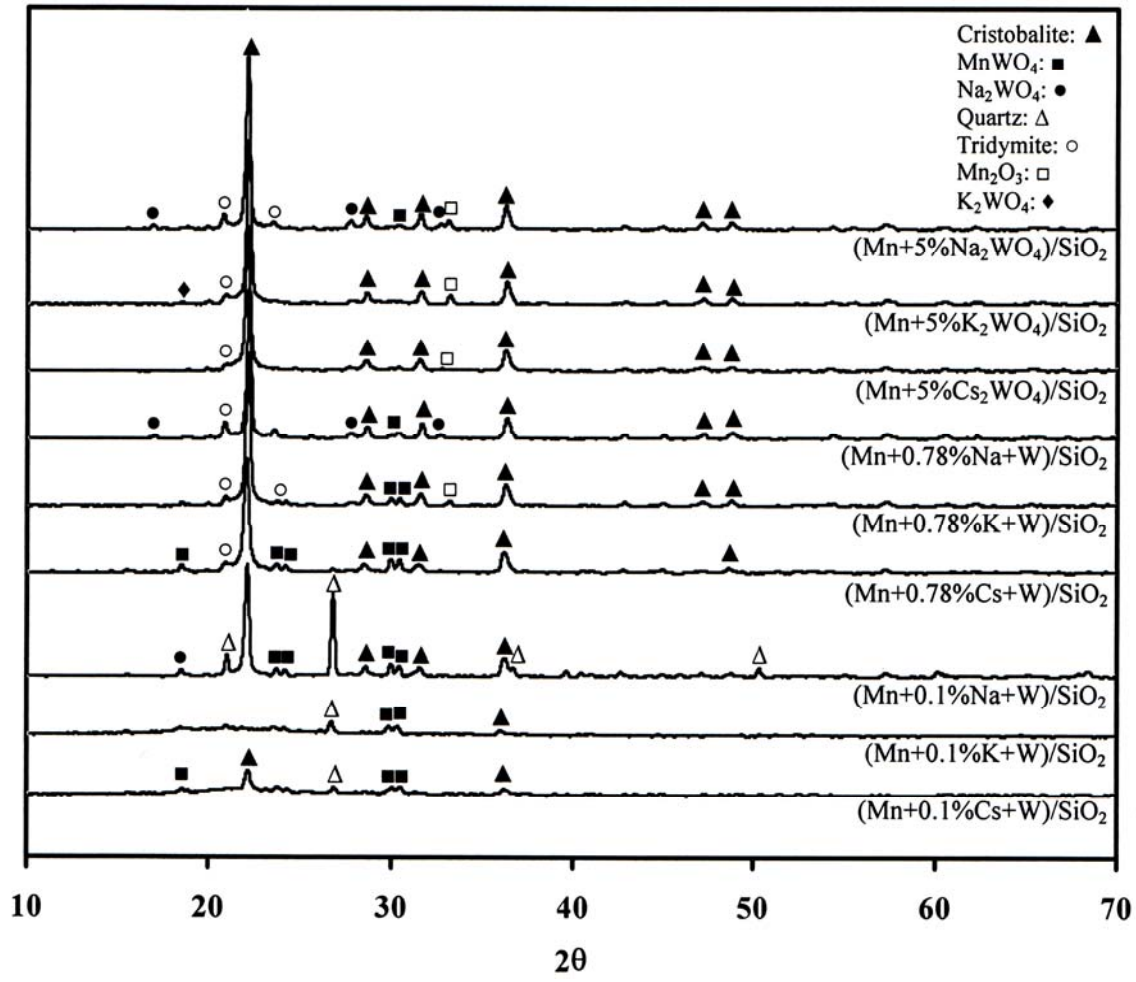

Fig. 3. XRD patterns of spent [4wt% Mn+(0.1 or 0.78)wt% (Na, K or Cs)+3.13wt% W]/SiO_2 and [4wt% Mn+5wt% (Na, K or Cs)$_2WO_4$]/SiO_2 catalysts after 12 h on OCM reaction conditions

Table 1. Crystallinity percent of fresh and spent [4wt%Mn+(0.1 or 0.78)wt%(Li, Na, K or Cs)+3.13wtW]/SiO_2 and [4wt%Mn+5wt%(Li, Na, K or Cs)$_2WO_4$]/SiO_2 catalysts

Catalyst	Fresh	Spent	Crystalline Phase and count		Crystallinity Percent	
			Cristobalite[a]	Quartz[b]	Cristobalite	Quartz
(4%Mn+3.13%W+0.1%Li)/SiO_2	√	-	√	√	34	4
	-	√	-	√	-	42
(4%Mn+5%Li_2WO_4)/SiO_2 (0.27%Li-3.5%W)	√	-	-	√	-	100[c]
	-	√	-	√	-	-
(4%Mn+3.13%W+0.78%Li)/SiO_2	√	-	-	√	-	74
	-	√	-	√	-	94
(4%Mn+3.13%W+0.1%Na)/SiO_2	√	-	√	-	13	-
	-	√	√	√	59	36
(4%Mn+3.13%W+0.78%Na)/SiO_2	√	-	√	-	100[d]	-
	-	√	√	-	-	-
(4%Mn+5%Na_2WO_4)/SiO_2 (0.78%Na-3.13%W)	√	-	√	-	100	-
	-	√	√	-	100	-

Table 1. (Continued)

(4%Mn+3.13%W+0.1%K)/SiO_2	√	-	√	-	7	-
	-	√	√	√	6	5
(4%Mn+3.13%W+0.78%K)/SiO_2	√	-	√	-	65	-
	-	√	√	-	77	-
(4%Mn +5%K_2WO_4)/SiO_2 (1.2%K -2.8%W)	√	-	√	-	81	-
	-	√	√	-	84	-
(4%Mn+3.13%W+0.1%Cs)/SiO_2	√	-	√	-	6	-
	-	√	√	-	14	-
(4%Mn+3.13%W+0.78%Cs)/SiO_2	√	-	√	-	7	-
	-	√	√	-	51	-
(4%Mn+ 5%Cs_2WO_4)/SiO_2 (2.6%Cs-1.8%W)	√	-	√	-	59	-
	-	√	√	-	71	-

[a]peak of 2θ = 26.9 is considered.
[b]peak of 2θ = 20.9 is considered.
[c]considered as reference to calculate crystallinity percent of catalysts containing lithium ion with quartz crystalline structure
[d]considered as reference to calculate crystallinity percent of catalysts containing sodium, potassium or cesium ions with cristobalite crystalline structure

Table 2. XRD data of fresh and spent SiO_2 supported catalysts that contain different weight percent of Na, W and Mn, reported in literature

Catalyst	Fresh	Spent	Crystalline phase of catalyst (SiO_2 support)			Crystalline phases of components						Ref.
			α–cristobalite	α–tridymite	Quartz	Na_2WO_4	$Na_2WO_4{\cdot}2H_2O$	$Na_2W_2O_7$	Mn_2O_3	$MnWO_4$	$MnMn_6SiO_{12}$	
(2%Mn+0.4%Na+3.13%W)/SiO_2	√	-	√	-	-	-	-	√	√	√	-	13
(2%Mn+0.8%Na+3.13%W)/SiO_2	√	-	√	-	-	√	-	√	√	-	-	
(2%Mn+0.8%Na+3.13%W)/SiO_2		√[a]	√	-	-	√	-	√	√	-	-	
(2%Mn+1.6%Na+3.13%W)/SiO_2	√	-	√	-	-	√	-	√	√	-	-	
(2%Mn+1.6%Na+3.13%W)/SiO_2		√[a]	√	-	-	√	-	√	√	-	-	
(2%Mn+2.3%Na+3.13%W)/SiO_2	√	-	√	-	-	√	-	√	√	-	-	
(2%Mn+4.6%Na+3.13%W)/SiO_2	√	-	√	-	-	√	-	√	√	-	-	
(2%Mn+7.8%Na+3.13%W)/SiO_2	√	-	√	-	-	√	-	√	√	-	-	
(2%Mn+0.8%Na+0.4%W)/SiO_2	√	-	√	-	-	√	-	√	√	-	-	
(2%Mn+0.8%Na+0.8%W)/SiO_2	√	-	√	-	-	√	-	√	√	-	-	
(2%Mn+0.8%Na+1.5%W)/SiO_2	√	-	√	-	-	√	-	√	√	-	-	
(2%Mn+0.8%Na+3..1%W)/SiO_2	√	-	√	-	-	√	-	√	√	-	-	
(2%Mn+0.8%Na+4.5%W)/SiO_2	√	-	√	-	-	√	-	√	√	-	-	
(2%Mn+0.8%Na+8.9%W)/SiO_2	√	-	√	-	-	√	-	-	-	√	-	
(2%Mn+0.8%Na+17.8%W)/SiO_2	√	-	√	-	-	-	-	-	-	√	-	
(0.5%Mn+0.8%Na+3.1%W)/SiO_2	√	-	√	-	-	√	-	√	√	-	-	
(1%Mn+0.8%Na+3.1%W)/SiO_2	√	-	√	-	-	√	-	√	√	-	-	
(2%Mn+0.8%Na+3.1%W)/SiO_2	√	-	√	-	-	√	-	√	√	-	-	
(3%Mn+0.8%Na+3..1%W)/SiO_2	√	-	√	-	-	√	-	√	√	-	-	
(6%Mn+0.8%Na+3.1%W)/SiO_2	√	-	√	-	-	√	-	√	√	-	-	
(12%Mn+0.8%Na+3.1%W)/SiO_2	√	-	√	-	-	√	-	√	√	√	-	
(24%Mn+0.8%Na+3.1%W)/SiO_2	√	-	√	-	-	√	-	√	-	√	√	
(2%Mn+5%Na_2WO_4)/SiO_2	√	-	√	-	-	√	-	-	√	-	-	15
(2%Mn+5%Na_2WO_4)/SiO_2	√[b]	-	-	√	√	-	-	-	√	-	-	
(2%Mn+5%Na_2WO_4)/SiO_2	-	√[c]	-	√	√	-	-	-	-	-	-	
(2%Mn+5%Na_2WO_4)/SiO_2	√[d]	-	√	-	√	√	-	-	√	-	-	17
(2%Mn+5%Na_2WO_4)/SiO_2	-	√[d]	-	√	√	√	-	-	√	-	-	
(2%Mn+5%Na_2WO_4)/SiO_2	√[e]	-	√	-	-	√	-	-	√	-	-	
(2%Mn+5%Na_2WO_4)/SiO_2	√[f]	-	√	-	-	√	-	-	√	-	-	

Table 2. (Continued)

$(4\%Mn+5\%Na_2WO_4)/SiO_2$	√	-	√	-	-	-	√	-	√	-	-	22
$(4\%Mn+5\%Na_2WO_4)/SiO_2$	-	√[g]	√	-	-	-	-	-	-	√	-	
$(2\%Mn+5\%Na_2WO_4)/SiO_2$		√[h]	√	-	-	-	-	-	-	√	-	
$(2\%Mn+5\%Na_2WO_4)/SiO_2$	√	-	√	-	-	√	√	√	√	√	-	21
$(2\%Mn+5\%Na_2WO_4)/SiO_2$	-	√	√	-	√	√	-	-	√	√	-	
$(2\%Mn+5\%Na_2WO_4)/SiO_2$	√	-	√	-	-	√	-	-	√	-	-	9
$5\%Na_2W_4/SiO_2$	√	-	√	-	-	√	-	-	-	-	-	
$(2\%Mn+5\%Na_2WO_4)/SiO_2$	√	-	√	-	-	√	-	√	√	-	-	16
$(2\%Mn+5\%Na_2WO_4)/SiO_2$	-	√	√	-	-	√	-	√	√	-	-	
$(2\%Mn+5\%Na_2WO_4)/SiO_2$	√	-	√	-	-	√	-	-	√	-	-	18
$(2\%Mn+5\%Na_2WO_4)/SiO_2$	-	√[i]	√	-	-	√	-	-	√	√	-	
$(Mn+Na_2WO_4)/SiO_2$	√	-	√	√	-	√	-		√	-	-	14
$(Mn+Na_2WO_4)/SiO_2$	-	√[j]	√	√	-	√	-	√	√	-	-	

[a]After 5 h OCM test
[b]After 500 h OCM test
[c]After 1000 h OCM test
[d]prepared by slurry method
[e]prepared by impregnation method
[f]prepared by sol-gel method
[g]After OCM test at 800°C
[h]After OCM test at 850°C
[i]After 4 h OCM test at 800°C
[j]After 8 h OCM test at 750°C

Table 3. XRD patterns of fresh and spent SiO_2 supported catalysts containing different weight percent of Mn, Li, K, Cs and W, reported in the literature

Catalyst	Fresh	Spent	Crystalline phase of catalyst (SiO_2 support)								Ref.
			α–cristobalite	α–tridymite	Quartz	Li_2WO_4	Li_6WO_6	K_2WO_4	Cs_2WO_4	Mn_2O_3	
(4%Mn+0.1%Li+3.1%W)/SiO_2	√[b]	-	√	-	-	-	-	-	-	-	16
(4%Mn+0.1%Li+3.1%W)/SiO_2	√[c]		√	-	-	-	-	-	-	-	
(4%Mn+0.1%Li+3.1%W)/SiO_2	-	√[d]	-	-	√	-	-	-	-	-	
(4%Mn+0.27%Li+3.1%W)/SiO_2[a]	√[b]	-	√	-	√	-	-	-	-	-	
(2%Mn+5%Li_2WO_4)/SiO_2	√	-	-	-	√	√	√	-	-	√	19
(2%Mn+5%Li_2WO_4)/SiO_2	-	√	-	-	√	√	√	-	-	√	
(2%Mn+5%K_2WO_4)/SiO_2	√	-	√	-	-	-	-	√	-	-	
(2%Mn+5%K_2WO_4)/SiO_2	-	√	√	-	-	-	-	√	-	-	
(2%Mn+5%Cs_2WO_4)/SiO_2	√	-	√	-	-	-	-	-	√	-	
(2%Mn+5%Cs_2WO_4)/SiO_2	-	√	√	-	-	-	-	-	√	-	

[a]Li and W weight percent are equal to the Li_2WO_4.
[b]After 8 h calcining at 800°C
[c]After 24 h OCM reaction at 800°C
[d]After 8 h OCM reaction at 800°C

Table 4. XRD data of fresh and spent SiO_2 supported catalysts, containing 4wt%Mn, 3.13wt%W and different wt% of alkali ions

Catalyst	Fresh[a]	Spent[b]	Crystalline phase of catalyst (SiO_2 support)					Crystalline phases of components				
			Cristobalite	Tridymite	Quartz	SiO_2	Li_2WO_4	Na_2WO_4	K_2WO_4	Mn_2O_3	$MnWO_4$	$Li_2Si_2O_5$
(Mn+0.1%Li+W)/SiO_2	√	-	√	√	√	√	-	-	-	√	√	-
	-	√	√	-	√	-	-	-	-	√	√	-
(Mn+0.1%Na+W)/SiO_2	√	-	√	√	-	-	-	-	-	√	√	-
	-	√	√	-	√	-	-	-	-	√	√	-
(Mn+0.1%K+W)/SiO_2	√	-	√	-	-	-	-	-	-	√	√	-
	-	√	√	-	-	-	-	-	-	√	√	-
(Mn+0.1%Cs+W)/SiO_2	√	-	√	√	-	-	-	-	-	√	√	-
	-	√	√	-	√	-	-	-	-	√	√	-
(Mn+0.78%Li+W)/SiO_2	√	-	√	√	√	-	√	-	-	√	√	-
	-	√	-	-	√	-	-	-	-	√	-	√
(Mn+0.78%Na+W)/SiO_2	√	-	√	√	-	-	-	√	-	√	√	-
	-	√	√	√	-	-	-	√	-	√	√	-
(Mn+0.78%K+W)/SiO_2	√	-	√	√	-	-	-	-	-	√	√	-
	-	√	√	√	-	-	-	-	√	√	√	-
(Mn+0.78%Cs+W)/SiO_2	√	-	√	-	-	-	-	-	-	√	√	-
	-	√	√	√	-	-	-	-	-	-	√	-
(Mn+5%Li_2W_4)/SiO_2 (0.27%Li+%W)	√	-	-	-	√	-	√	-	-	√	-	-
	-	√	-	-	√	-	-	-	-	√	√	-
(4%Mn+5%Na_2W_4)/SiO_2 (0.78%Li+3.13%W)	√	-	√	√	-	-	-	√	-	√	-	-
	-	√	√	√	-	-	-	√	-	√	√	-
(4%Mn+5%K_2W_4)/SiO_2 (2.1%K+%W)	√	-	√	√	-	-	-	-	√	√	-	-
	-	√	√	√	-	-	√	-	√	√	-	-
(4%Mn+5%Cs_2W_4)/SiO_2 (2.6%Li+%W)	√	-	√	√	-	-	-	-	-	√	-	-
	-	√	√	√	-	-	-	-	-	√	-	-

[a]after 8 h calcinig at 800^{o}C

[b]after 12 h on OCM reaction condition

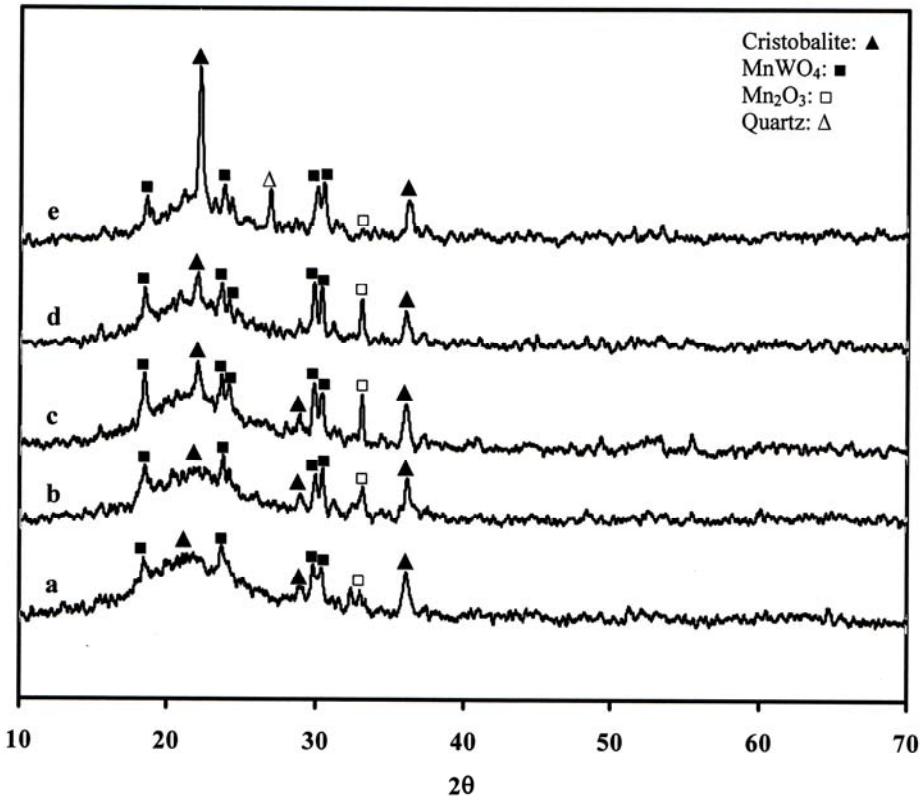

Fig. 4. XRD Patterns of catalysts containing Cs ion; a and b: fresh (Mn+0.1wt%Cs+W)/SiO_2 samples after 8 h calcination under air atmosphere at 800 and 900°C, respectively; c and d: fresh (Mn+0.78wt%Cs+W)/SiO_2 samples 8 h calcination under air atmosphere at 800 and 900°C, respectively; e: spent (Mn+0.1wt% Cs+W)/SiO_2 catalyst after 12 h on OCM reaction

Increase in crystallinty of the catalysts under the OCM reaction, however, is evidence for new conditions for higher degree of crystallinty. The structural flexibility of the catalysts is accordingly suggested as the property of OCM reaction condition and is accounted as the main chemical role of the alkali ion. It can be related to the amorphous silica phase transition in the presence of alkali ions, especially in the form of tungstate. Appearance of the non-bridging oxygen during the crystallization of silica in the presence of alkali tungstate is accompanied by the incorporation of the tungstate in silica lattice. Tetrahedral WO_4^{2-} surface species, having one W=O and three W-O-Si surface bonds are known as the OCM active sites [16-17]. Thus the structural flexibility is proposed to take place by the Si-O and Si–O–W bond breaking in the presence of an alkali ion, especially under the OCM reaction condition, which results in much more mobility of the surface and lattice oxygens [11].

The crystallite size of the catalyst components, reported in the literature and obtained in this work, is compared in Table 5. The results were calculated by the Scherrer equation using XRD spectra. Small change is observed for the crystallite size of the fresh and spent catalysts. Results are in good agreement with the SEM images, in which similar morphology is observed for the crystalline catalysts containing different alkali ions (Fig. 5). The crystallite size is observed to increase by having quartz as the final crystalline structural.

Porous silica is a nonselective material for the OCM reaction [9-10, 13, 16-17]. Crystallization makes the silica support and the catalysts nonporous, a feature that drastically reduces the surface area. The crystallized nonporous silica is an inactive material with respect to OCM reaction. The results of the catalysts performance and the conductivity measurements under oxidizing atmosphere and under OCM reaction condition are shown in Tables 6 and 7. Compared to the amorphous porous silica support, the un–crystallized catalysts containing alkali ion are observed to be selective for the OCM reaction. XRD analysis and the results presented in Table 6 also show that the crystalline phase is not an important parameter for the formation of an active / selective catalyst [16, 19]. The presence of alkali ion, however, is an important parameter for the formation of an active / selective catalyst. This is

due to the structural flexibility that is provided by the presence of the alkali ion and is accompanied by the catalyst phase transition. Moles of the alkali ion required for the formation of alkali tungstate provide the best conditions for crystallization during the calcination in air, providing a more active / selective OCM catalyst.

Fourier transformed infrared (FTIR) spectroscopy results of the amorphous silica, the fresh and spent SiO_2 supported tri–metallic catalysts in the range of 400–1600 cm^{-1} are shown in Figs. 6-8. The results for mono and bi–metallic catalysts with no alkali ion are similar to thoes of the amorphous silica (data not shown). The results of this work, compared with those reported in the literature are shown in Table 8. The basic site of the catalyst, the IR bands of the metal tungstate and manganese species cannot be detected in the FTIR spectra of the fresh and the used Na–W–Mn/SiO_2 catalysts [16-21]. The IR bands of amorphous SiO_2, α–cristobalite and quartz, however, are distinguished. Accordingly the interaction of tetrahedral WO_4 and octahedral WO_6 with the support in the catalysts was inferred from the changes in the IR spectra of SiO_2. The FTIR results of the spent catalysts indicate that the tetrahedral WO_4 are stable with α–cristobalite [18]. The FTIR results of the fresh and spent Li–W–Mn/SiO_2 catalyst, however, showed that the interaction of the tetrahedral WO_4 with the quartz is weak and the tetrahedral WO_4 is unstable in this system [16]. Significant differences observed between the amorphous silica, cristobalite and quartz are not distinguished for the crystalline forms.

Temperature programmed reduction investigations of the spent catalysts containing different loading of the alkali ions are shown in Figs. 9 and 10. Manganese species that are formed during the catalysts preparation depend on the manganese loading, support and calcinations temperature [24-26]. Mn_2O_3 was detected as the manganese species in all the prepared catalysts (Figs. 1-3 and Table 4). Reduction patterns of the bulk $MnO_{1.5}$ were associated with the reduction states of $Mn_2O_3 \rightarrow Mn_3O_4 \rightarrow MnO$, respectively [26-29]. Reduction of MnO to metallic Mn was reported to be quite unlikely based on the thermodynamic considerations and experimental evidence from the literature [26-27]. The broad reduction feature of the manganese species, observed in [Mn+0.1wt%(Na, K or Cs)+W]/SiO_2 and (Mn+5wt%Cs_2WO_4)/SiO_2 catalysts, is attributed to the low crystallinity of the manganese oxide in these samples (see Fig. 3). The crystallite size of the manganese species was not accordingly detected (see Table 5).

Table 5. Crystallite size[a] of different components in fresh and spent trimetallic catalysts, containing Mn, W and an alkali ion

Catalyst	Fresh	Spent	crystallite size of the catalyst components(nm)			Refrence
			Cristobalite	Quartz	Mn_2O_3	
$(2\%Mn+Li_2WO_4)/SiO_2$	√	-	-	-	139	16
	-	√	-	-	146	
$(2\%Mn+Na_2WO_4)/SiO_2$	√	-	-	-	87	
	-	√	-	-	89	
$(2\%Mn+K_2WO_4)/SiO_2$	√	-	-	-	58	
	-	√	-	-	61	
$(2\%Mn+Na_2WO_4)/SiO_2$	-	-	-	-	61.4	17
	-	-	-	-	56.8	
	-	-	-	-	82.1	
$(4\%Mn+Na_2WO_4)/SiO_2$	-	-	-	-	18.2	22
$(4\%Mn+0.1\%Li+3.13\%W)/SiO_2$	√	-	-	-	-	This Work
	-	√	-	65.32	-	
$(4\%Mn+0.1\%Na+3.13\%W)/SiO_2$	-	√	44.40	-	-	
$(4\%Mn+0.78\%Li+3.13\%W)/SiO_2$	√	-	-	70.08	70.58	
	-	√	-	73.51	72.57	
$(4\%Mn+0.78\%Na+3.13\%W)/SiO_2$	√	-	55.83	-	64.91	
	-	√	58.86	-	71.28	
$(4\%Mn+0.78\%K+3.13\%W)/SiO_2$	√	-	45.21	-	-	
	-	√	45.37	-	-	
$(4\%Mn+5\%Li_2WO_4)/SiO_2$	√	-	-	71.24	71.69	
	-	√	-	72.27	78.69	
$(4\%Mn+5\%Na_2WO_4)/SiO_2$	√	-	54.07	-	64.16	
	-	√	58.72	-	71.46	
$(4\%Mn+5\%K_2WO_4)/SiO_2$	√	-	46.43	-	53.13	
	-	√	47.58	-	58.42	
$(4\%Mn+5\%Cs_2WO_4)/SiO_2$	√	-	39.85	-	-	
	-	√	36.34	-	-	

[a]Data of the literature and this work were calculated using Scherrer equation according to the XRD results.

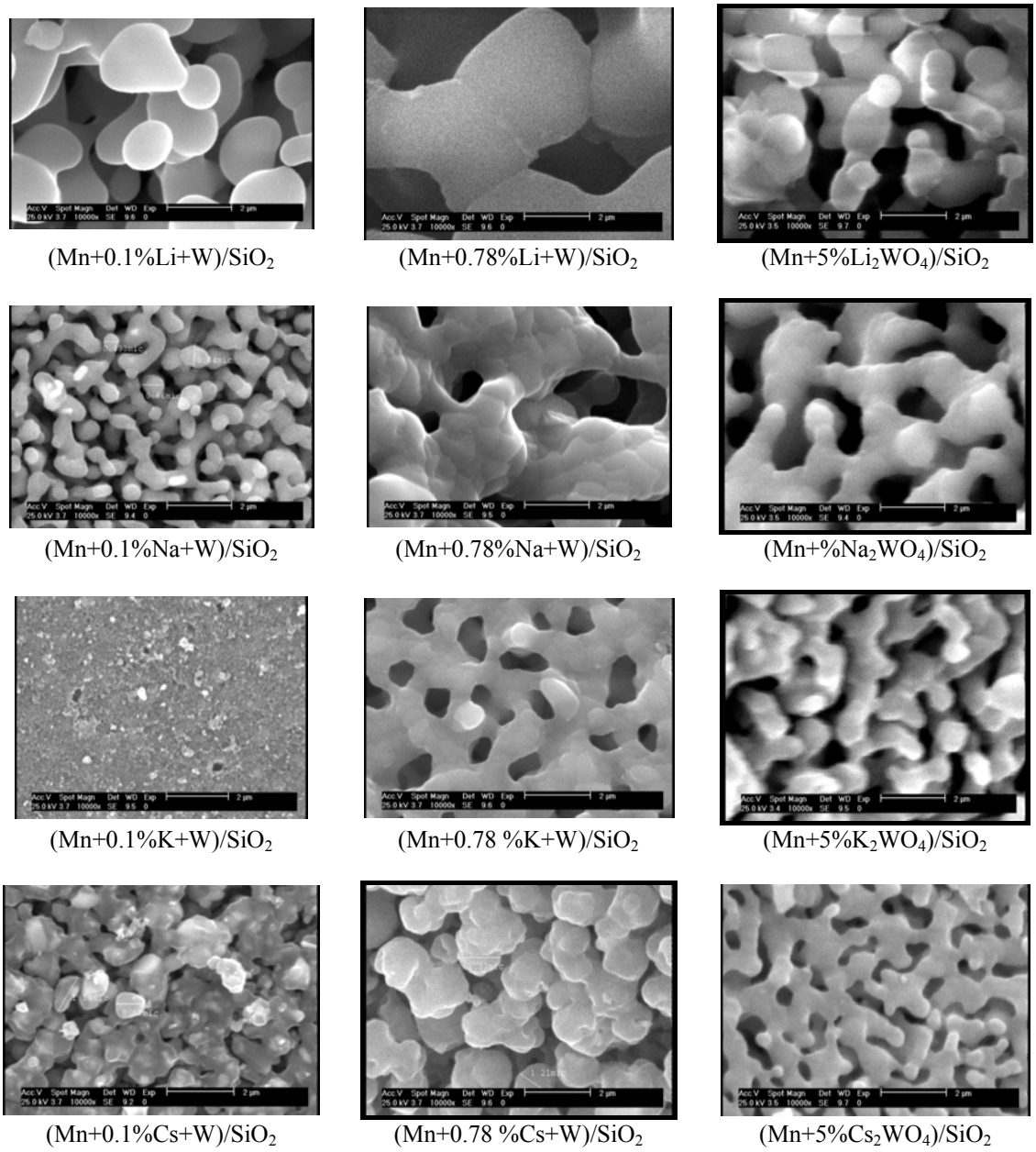

Fig. 5. SEM results of spent [4wt%Mn+(0.1 or 0.78)wt%(Li, Na, K or Cs)+3.13wt%W)/SiO_2 and [4wt%Mn+5wt%(Li, Na, K or Cs)$_2WO_4$]/SiO_2 catalysts

Table 6. Oxidative Coupling of Methane performance and electrical conductivity measurement results over [4wt%Mn+(0.1 or 0.78)wt% (Li, Na, K or Cs)+3.13wt%W]/SiO_2 and [4wt%Mn+5wt%(Li, Na, K or Cs)$_2WO_4$]/SiO_2 catalysts under different conditions[a]

Catalyst	Oxidant	C (mol%)	S	$\frac{C_2H_4}{C_2H_6}$	Y	C+S	$\sigma_{Ox.}$[b] (MΩ)	$\frac{\sigma_{OCM}}{\sigma_{Ox.}}$[c]
(Mn+0.1wt%Li+W)/SiO_2	Air	29	76	1.5	21	102	6.78	2
	O_2	27	70	1.9	19	98	0.32	2655
(Mn+0.1wt%Na+W)/SiO_2	Air	32	71	1.7	23	102	0.33	450
	O_2	28	71	1.8	20	100	1	46818
(Mn+0.1wt%K+W)/SiO_2	Air	27	62	1.2	17	89	1.38	1
	O_2	25	63	1.8	16	88	1.56	2166
(Mn+0.1wt%Cs+W)/SiO_2	Air	28	63	1.4	18	91	1.58	1
	O_2	28	70	1.8	19	98	1.50	10695
(Mn+0.78wt%Li+W)/SiO_2	Air	17	76	1.1	13	93	0.35	1
	O_2	19	77	1.2	15	96	1.8	1
(Mn+0.78wt%Na+W)/SiO_2	Air	31	78	1.8	24	108	1.13	3
	O_2	34	68	2.4	23	102	1.22	105455
(Mn+0.78wt%K+W)/SiO_2	Air	31	75	1.4	23	106	1.38	2
	O_2	33	71	1.8	23	104	0.69	105907
(Mn+0.78wt%K+W)/SiO_2	Air	29	66	1.7	19	95	1.38	13
	O_2	27	67	2.2	18	95	1.33	134793
(Mn+Li_2WO_4)/SiO_2 (Mn+0.27wt%Li+W)/SiO_2	Air	24	84	1.2	20	106	1.50	6
	O_2	36	64	2.4	20	95	1.50	156
(Mn+Na_2WO_4)/SiO_2 (Mn+0.78wt%Li+3.13wt%W)/SiO_2	Air	36	71	2	26	107	1.50	27
	O_2	35	71	2.3	24	104	2.33	2857
(Mn+K_2WO_4)/SiO_2 (Mn+2.1wt%K+W)/SiO_2	Air	28	74	1.7	21	102	0.67	38
	O_2	29	67	2.1	19	96	0.43	9333
(Mn+Cs_2WO_4)/SiO_2 (Mn+2.6wt%Cs+W)/SiO_2	Air	31	61	1.6	19	92	0.25	27
	O_2	32	58	2.3	18	90	0.75	7188

[a] $\frac{CH_4}{air}=\frac{1}{1}$ or $\frac{CH_4}{O_2}=\frac{5}{1}$, feed flow rate of 112 mL/min (STP), GHSV=13200 mL/g_{Cat}·h, 800°C

[b] $\sigma_{Ox.}$ is denoted for conductivity under the oxidant atmosphere at 800°C.

[c] σ_{OCM} is denoted for conductivity under the OCM reaction conditions.

Table 7. Oxidative Coupling of Methane performance and electrical conductivity measurement results over 4wt%Mn/SiO_2, 3.13wt% W/SiO_2, (3.13wt%W+4wt%Mn)/SiO_2 and 5wt%Na_2WO_4/SiO_2 catalysts under different conditions[a]

Catalyst	Oxidant	C (mol%)	S	$\frac{C_2H_4}{C_2H_6}$	Y	C+S	$\sigma_{Ox.}$[b] (MΩ)	$(\sigma_{OCM}/\sigma_{Ox})$[c]
4wt%Mn/SiO_2	Air	24	57	1.2	13	80	2.03	0.7
	O_2	26	50	1.7	13	76	1.50	1.04
3.13wt%W/SiO_2	Air	13	62	0.8	8	75	2	1
	O_2	14	46	0.9	6	60	2.85	1.25
(4wt%Mn+3.13wt%W)/SiO_2	Air	25	58	1.2	14	83	2.2	1.1
	O_2	27	49	1.9	13	76	0.43	1.56
5wt%Na_2WO_4/SiO_2	Air	28	62	2.5	18	93	1.44	250.86
	O_2	24	74	1.9	18	98	3	2.3

[a] CH_4/air = 1 or CH_4/O_2 = 5, feed flow rate of 112 mL/min (STP), GHSV=13200 mL/g_{Cat}·h, 800°C
[b] $\sigma_{Ox.}$ is denoted for conductivity under the oxidant atmosphere at 800°C.
[c] σ_{OCM} is denoted for conductivity under the OCM reaction conditions.

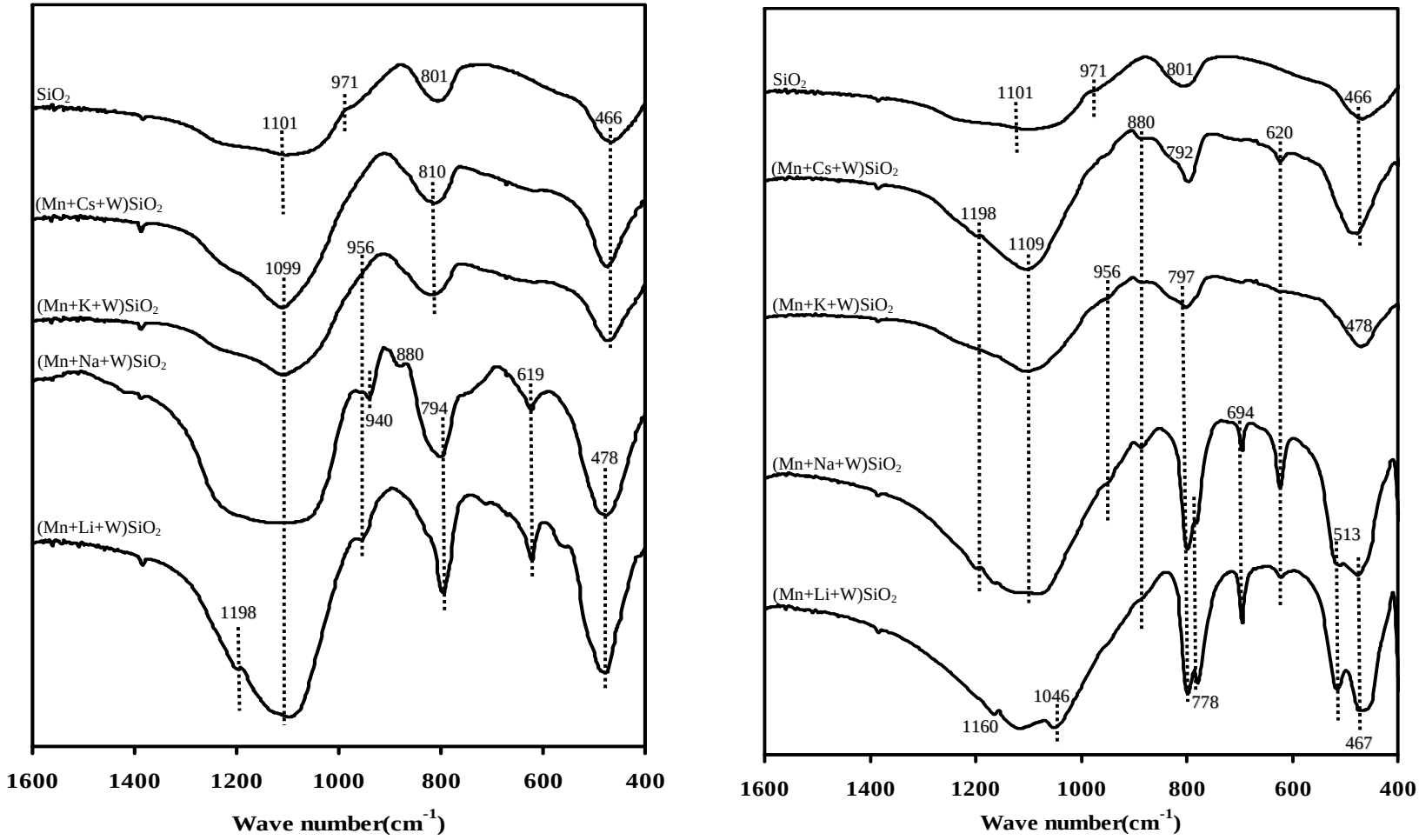

Fresh [Mn+0.1wt%(Li, Na, K, Cs)+W)/SiO_2 Spent [Mn+0.1wt%(Li, Na, K, Cs)+W)/SiO_2

Fig. 6. FTIR results of fresh and spent [4wt%Mn+0.1wt%(Li, Na, K, Cs)+3.13wt%W)/SiO_2

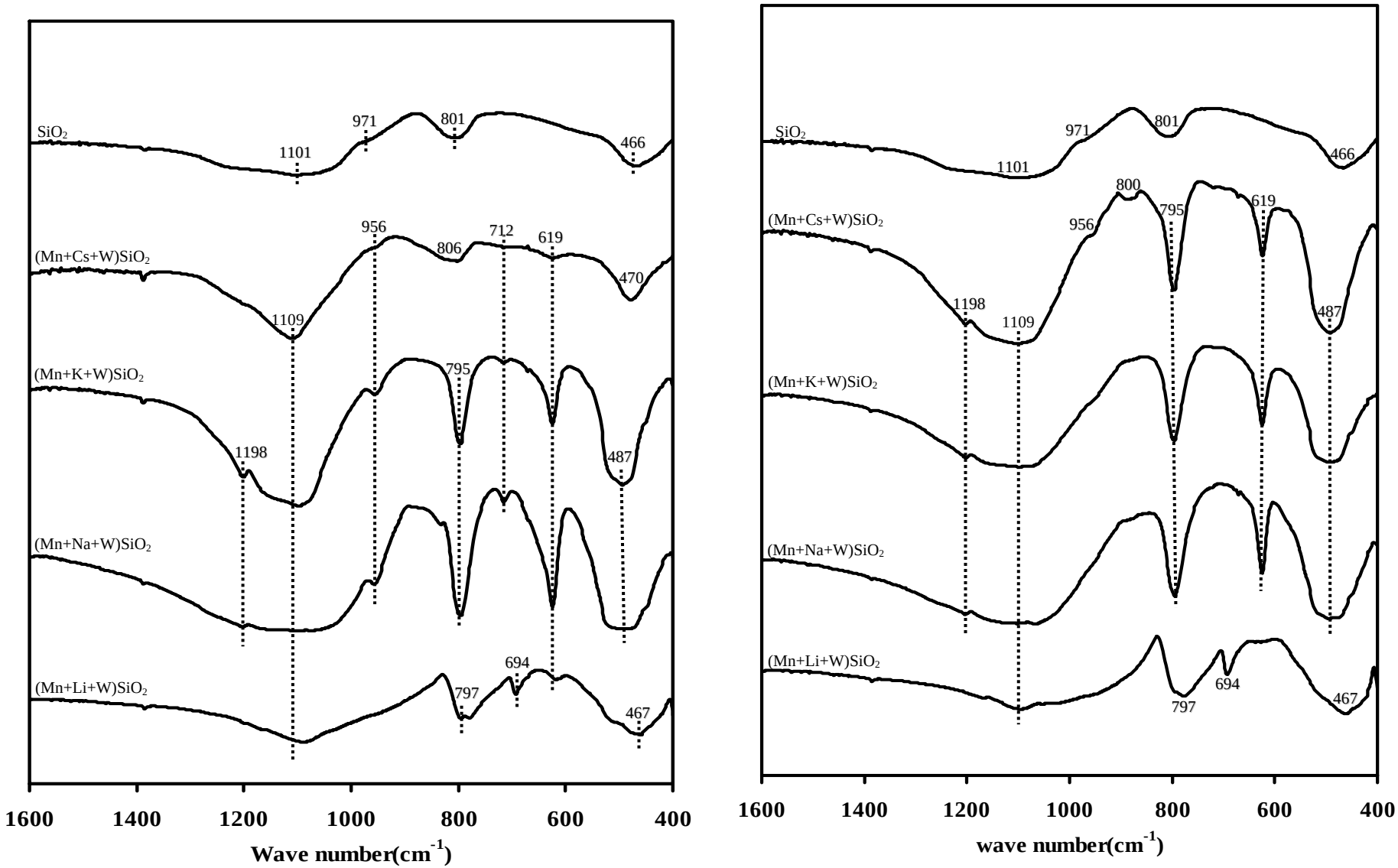

Fresh [Mn+0.78wt%(Li, Na, K or Cs)+W]/SiO_2 Spent [Mn+0.78wt%(Li, Na, K or Cs)+W]/SiO_2

Fig. 7. FTIR results of fresh and spent [4wt%Mn+0.78wt%(Li, Na, K or Cs)+3.13wt%W)/SiO2 catalysts

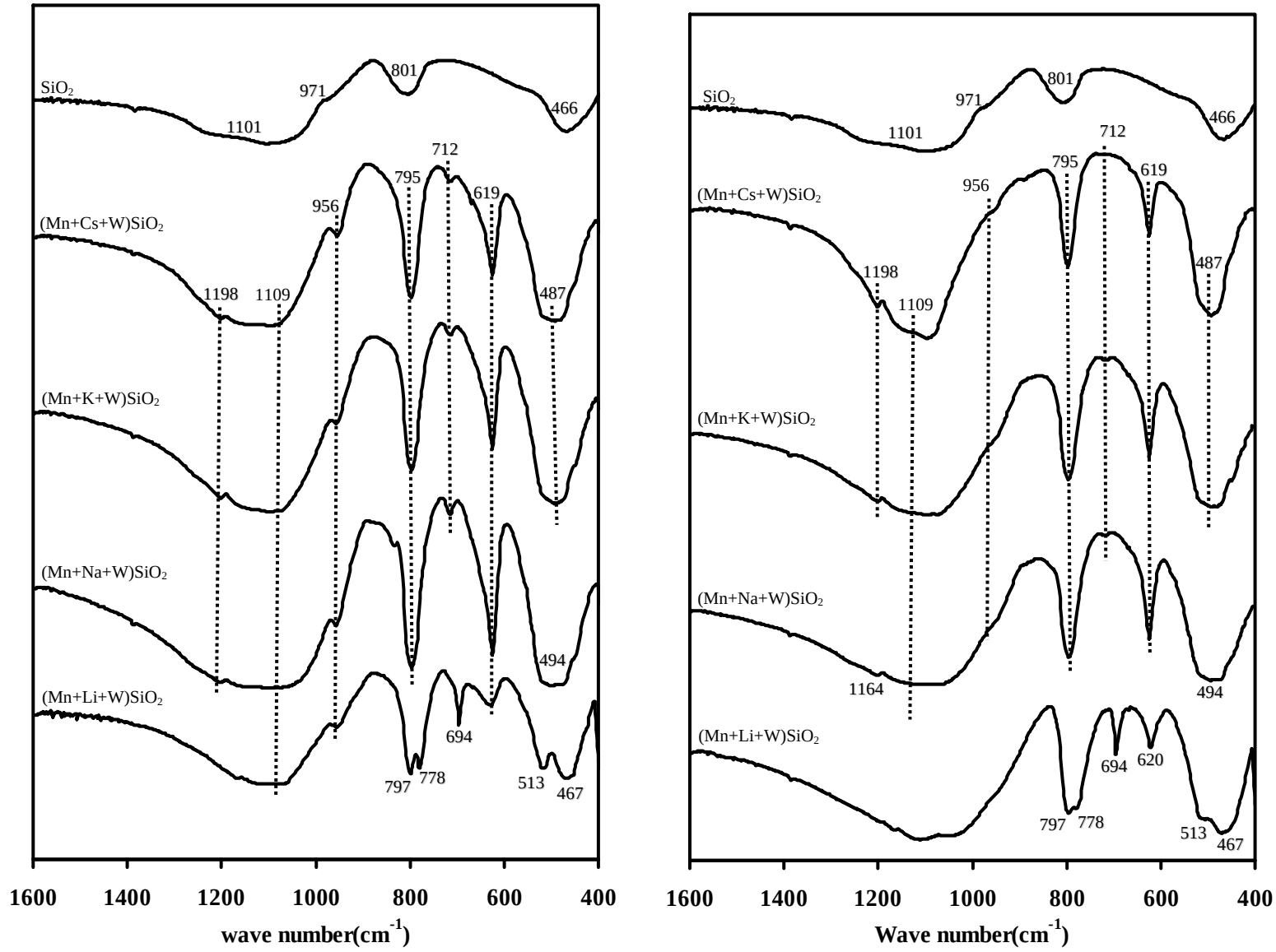

Fresh $[Mn+5wt\%(Li, Na, K, Cs)_2WO_4]/SiO_2$ Spent $[Mn+5wt\%(Li, Na, K, Cs)_2WO_4]/SiO_2$

Fig. 8. FTIR results of fresh and spent $[4wt\%Mn+5wt\%(Li, Na, K, Cs)_2WO_4]/SiO_2$ catalysts

Table 8. FT-IR data of the samples

Sample	Fresh	Spent	Peak position (cm^{-1})										Ref.
Amorphous SiO_2	-	-	466	-	-	801	-	971	1101	-	-	-	16
	-	-	466	-	-	801	-	971	1101	-	-	-	This work
α–cristobalite	-	-	483	619	-	793	-	-	1092	1200	-	-	16
Fresh Na-W-Mn/SiO_2[a]	√	-	484	622	713	797	856	957	1079	1133	1883	3325	21
Na-W-Mn/SiO_2[a]	√	-	494	619	-	795	-	-	1099	1198	-	-	16
	-	√	494	619	-	795	-	-	1099	1198	-	-	
K–W–Mn/SiO_2[a]	√	-	487	619	-	795	-	-	1099	1198	-	-	
	-	√	487	619	-	795	-	-	1099	1198	-	-	
Li–W–Mn/SiO_2[b]	√	-	470	513	694	778	797	1057	1099	1164	-	-	
	-	√	470	513	694	778	797	1049	1099	1164	-	-	
(Mn+0.1%Li+W)/SiO_2	√[a]	-	476	619	794	-	956	-	1099	1198	-	-	This work
	-	√[b]	467	513	620	694	778	797	880	-	1046	1160	
(Mn+0.1%Na+W)/SiO_2[a]	√	-	476	619	794	880	940	956	-	1099	-	-	
	-	√	467	513	620	694	778	797	880	956	1099	1198	
(Mn+0.1%K+W)/SiO_2[c]	√	-	466	-	-	810	-	956	1099	-	-	-	
	-	√	478	620	797	-	-	956	1099	1198	-	-	
(Mn+0.1%Cs+W)/SiO_2[c]	√	-	466	-	-	810	-	-	1099	-	-	-	
	-	√	466	620	792	880	-	-	1099	1198	-	-	
(Mn+0.78%Li+W)/SiO_2[b]	√	-	467	513	619	694	778	797	1099	1198	-	-	
	-	√	467	-	-	694	778	797	1099	1198	-	-	
(Mn+0.78%Na+W)/SiO_2[a]	√	-	487	619	712	795	956	-	1099	1198	487	619	
	-	√	487	619	795	880	956	-	1099	1198	-	-	
(Mn+0.78%K+W)/SiO_2[a]	√	-	487	619	712	795	956	-	1099	1198	-	-	
	-	√	487	619	795	880	956	-	1099	1198	-	-	
(Mn+0.78%Cs+W)/SiO_2[a]	√	-	470	619	712	806	956	-	1099	-	-	-	
	-	√	487	619	795	880	956	-	1099	1198	-	-	
(Mn+5%Li_2WO_4)/SiO_2[b]	√	-	467	513	620	694	778	797	956	1099	1164	-	
	-	√	467	513	620	694	778	797	956	1099	1164	-	
(Mn+5%Na_2WO_4)/SiO_2[a]	√	-	494	619	712	795	-	956	1099	1164	-	-	
	-	√	494	619	712	795	-	956	1099	1164	-	-	
(Mn+5%K_2WO_4)/SiO_2[a]	√	-	487	619	712	795	-	956	1099	1198	-	-	
	-	√	487	619	712	795	-	956	1099	1198	-	-	
(Mn+5%Cs_2WO_4)/SiO_2[a]	√	-	487	619	712	795	-	956	1099	1198	-	-	
	-	√	487	619	712	795	-	956	1099	1198	-	-	

[a]α–cristobalite
[b]quartz
[c]amorphous

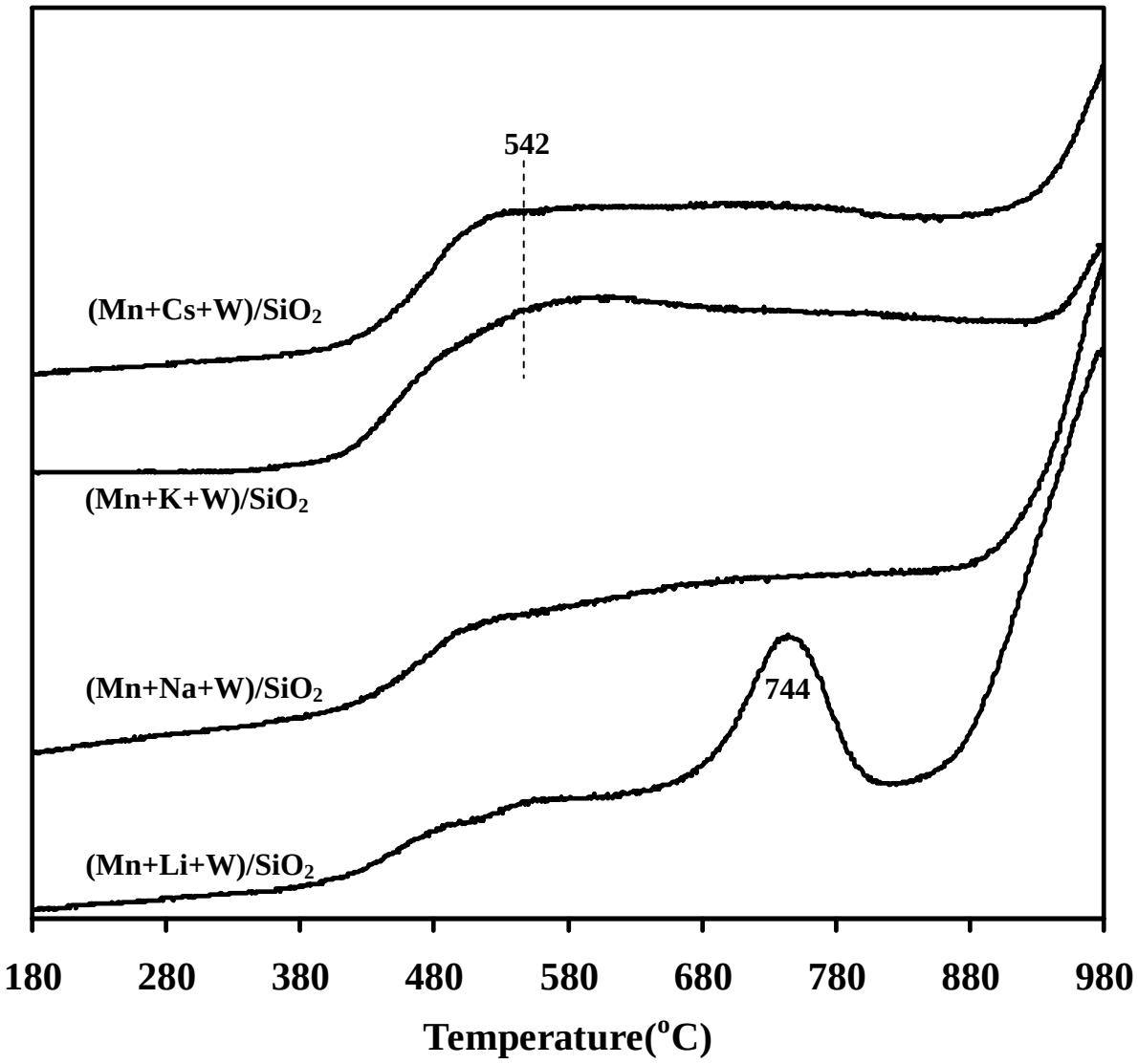

Fig. 9. TPR results of spent [4wt%Mn+0.1wt%(Li, Na, K or Cs)+3.13wt%W)/SiO_2 catalysts after 10 h on OCM reaction

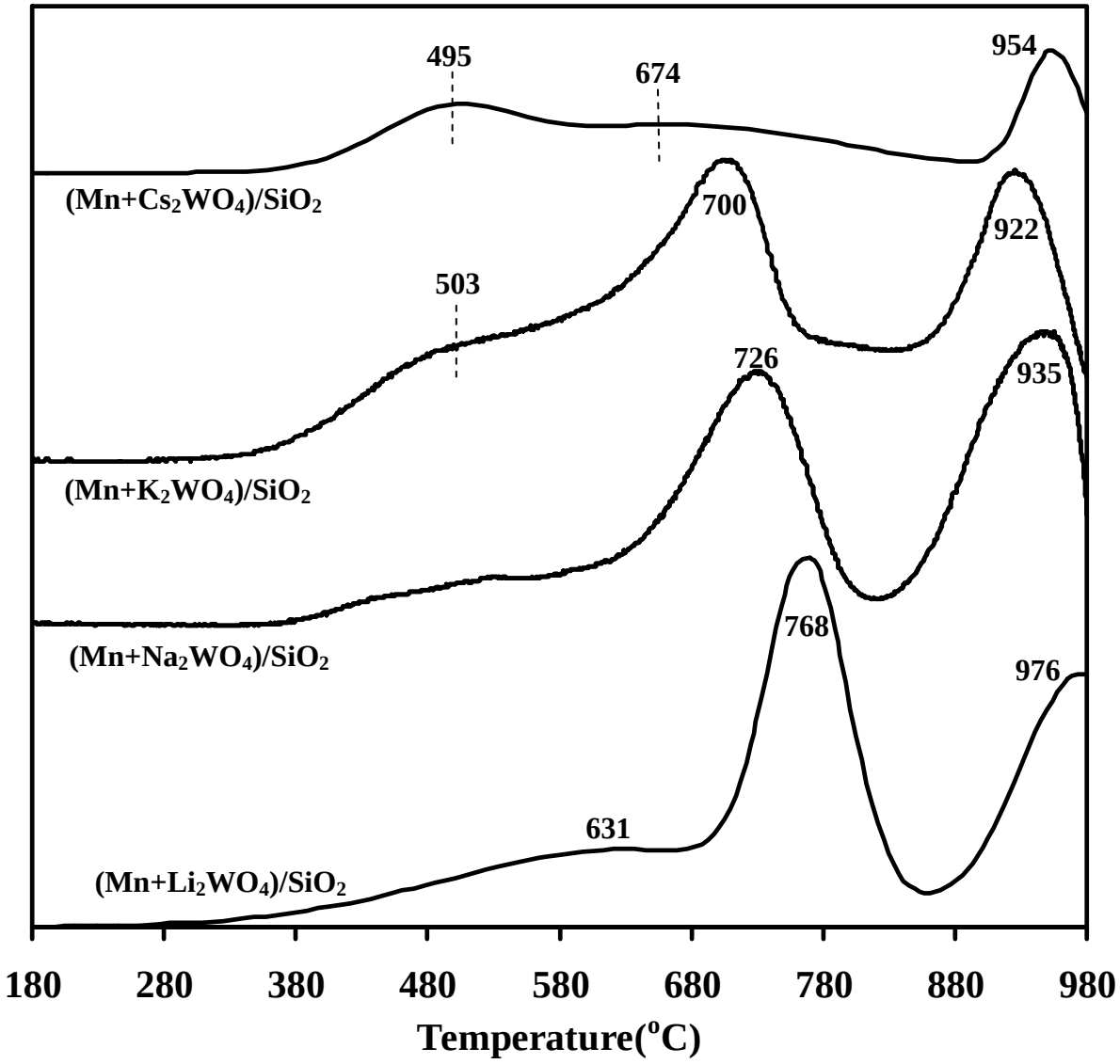

Fig. 10. TPR results of spent [4wt%Mn+5wt%(Li, Na, K or Cs)$_2$WO$_4$]/SiO$_2$ catalysts after 10 h on OCM reaction

4. Conclusion

The investigation of the oxidative coupling of methane reaction over catalysts containing different amounts of alkali ions, i.e. Li, Na, K and Cs, shows that catalyst crystalline phase is not an important parameter for the formation of an active or selective catalyst. The Crystallinty of a catalyst containing an alkali ion increases in the course of the OCM reaction. New conditions which are provided under the OCM reaction cause the phase transition of the catalyst containing alkali ions. This introduces a kind of structural flexibility of the catalyst under the reaction conditions. This structural flexibility is considered the main chemical role of alkali ions.

References

[1] Gao, Z. & Shi, Y. (2010). Suppressed formation of CO_2 and H_2O in the oxidative coupling of methane over La_2O_3/MgO catalyst by surface modification. *J. Nat. Gas Chem., 19*, 173-178.

[2] Production: Growth is the Norm. (2006). Chemical and Engineering News. 59-68.

[3] Rostrup-Nielsen, J. R. (1984). Catalytic Steam Reforming, in: J. R. Anderson, M. Boudart (Eds.), *Catalysis Science and Technolog.* Berlin, *5*, (Chapter 1), Springer.

[4] Zhang, J., Burkle-Vitzthum, V., Marquaire, P. M., Wild, G. & Commenge, J. M. (2011). Direct conversion of methane in formaldehyde at very short residence time. *Chem. Eng. Sci., 66*, 6331-6340.

[5] Holmen, A. (2009). Direct conversion of methane to fuels and chemicals. *Catal. Today, 142*, 2-8.

[6] Baidya, T., Vegten, N. V., Jiang, Y., Krumeich, F. &

Baiker, A. (2011). Oxidative coupling of methane over Ca- and alkali metal-doped ThO_2. *Appl. Catal. A: General., 391*, 205-214.

[7] Jiang, Z., Yu, C., Fang, X., Li, S. & Wang, H. (1993). Oxide/support interaction and surface reconstruction in the sodium tungstate(Na_2WO_4)/silica system. *J. Phys. Chem., 97,* 12870-12875.

[8] Wang, D., Rosynek, M. P. & Lunsford, J. H. (1995). Oxidative Coupling of Methane over Oxide-Supported Sodium-Manganese Catalysts. *J. Catal., 155,* 390-402.

[9] Palermo, A., Vazquez, J. P. H., Lee, A. F., Tikhov, M. S. & Lambert, R. M. (1998). Critical influence of the amorphous silica-to-cristobalite phase transition on the performance of $Mn/Na_2WO_4/SiO_2$ catalysts for the oxidative coupling of methane. *J. Catal., 177*, 259-266.

[10] Palermo, A., Vazquez, J. P. H. & Lambert, R. M. (2000). New efficient catalysts for the oxidative coupling of methane. *Catal. Lett., 68,* 191-196.

[11] Malekzadeh, A., Khodadadi, A., Abedini, M., Amini, M., Bahramian, A. & Dalai, A. K. (2001). Correlation of electrical properties and performance of OCM $MO_x/Na_2WO_4/SiO_2$ catalysts. *Cat. Comm., 2,* 241-247.

[12] Malekzadeh, A., Abedini, M., Khodadadi, A., Amini, M., Mishra, H. K. & Dalai. A. K. (2002). Critical Influence of Mn on Low-Temperature Catalytic Activity of $Mn/Na_2WO_4/SiO_2$ Catalyst for Oxidative Coupling of Methane. *Cat. Lett., 84,* 45-51.

[13] Ji, S., Xiao, T., Li, S., Xu, C., Hou, R., Coleman, K. S. & Green, M. L. H. (2002). The relationship between the structure and the performance of Na-W-Mn/SiO_2 catalysts for the oxidative coupling of methane. *Appl. Catal. A., 225,* 271-284.

[14] Chou, L., Cai, Y., Zhang, B., Niu, J., Ji, S. & Li, S. (2002). Oxidative Coupling of Methane over Na-W-Mn/SiO_2 Catalysts at Elevated Pressures. *J. Nat. Gas Chem., 11,* 131-136.

[15] Li, S. (2003). Reaction Chemistry of W-Mn/SiO_2 Catalyst for the Oxidative Coupling of Methane. *J. Nat. Gas Chem., 12,* 1-9.

[16] Ji, S., Xiao, T., Li, S., Chou, L., Zhang, B., Xu, C., Hou, R., York, A. P. E. & Green, M. L. H. (2003). Surface WO_4 tetrahedron: the essence of the oxidative coupling of methane over M-W-Mn/SiO_2 catalysts. *J. Catal., 220,* 47-56.

[17] Wang, J., Chou, L., Zhang, B., Song, H., Zhao, J., Yang, J. & Li, S. (2006). Comparative study on oxidation of methane to ethane and ethylene over Na_2WO_4–Mn/SiO_2 catalysts prepared by different methods. *J. Mol. Catal A: Chem., 245,* 272-277.

[18] Hou, S., Cao, Y., Xiong, W., Liu, H. & Kou, Y. (2006). Site Requirements for the Oxidative Coupling of Methane on SiO_2-Supported Mn Catalysts. *Ind. Eng. Chem. Res., 45*(21), 7077-7083.

[19] Malekzadeh, A., Khodadadi, A., Dalai, A. K. & Abedini, M. (2007). Oxidative Coupling of Methane over Lithium Doped (Mn+W)/SiO_2 Catalysts. *J. Nat. Gas Chem., 16,* 121-129.

[20] Malekzadeh, A., Dalai, A. K., Khodadadi, A. & Y. Mortazavi. (2008). Structural features of Na_2WO_4–MO_x/SiO_2 catalysts in oxidative coupling of methane reaction. *Cat. Comm., 9,* 960-965.

[21] Chua, Y. T., Mohamed, A. R. & Bhatia, S. (2008). Oxidative coupling of methane for the production of ethylene over sodium-tungsten-manganese-supported-silica catalyst (Na-W-Mn/SiO_2). *Appl. Catal A: General., 343,* 142-148.

[22] Salehoun, V., Khodadadi, A., Mortazavi, Y. & Talebizadeh. A. (2008). Dynamics of $Mn/Na_2WO_4/SiO_2$ catalyst in oxidative coupling of methane. *Chem. Eng. Sci., 63,* 4910-4916.

[23] Gholipour, Z., Malekzadeh, A., Hatami, R., Mortazavi, Y. & Khodadadi, A. (2010). Oxidative coupling of methane over (Na_2WO_4+Mn or Ce)/SiO_2 catalysts: In situ measurement of electrical conductivity. *J. Nat. Gas Chem., 19,* 35-42.

[24] Craciun, R., Nentwick, B., Hadjiivanov, K. & Knözinger, H. (2003). Structure and redox properties of MnO_x/Yttrium-stabilized zirconia (YSZ) catalyst and its used in CO and CH_4 oxidation. *Appl. Catal. A: General., 243*, 67-79.

[25] Ramesh, K., Chen, L., Chen, F., Liu, Y., Wang, Z. & Han, Y. F. (2008). Re-investigating the CO oxidation mechanism over unsupported MnO, Mn_2O_3 and MnO_2 catalysts. *Catal. Today., 131,* 477-482.

[26] Arena, F., Torre, T., Raimondo, C. & Parmaliana, A. (2001). Structure and redox properties of bulk and supported manganese oxide catalysts. *Phys. Chem. Chem. Phys. (PCCP), 3,* 1911-1917.

[27] Kapteijn, F., Singoredjo, L., Andreini, A. & Moulijn, J. A. (1994). Activity and selectivity of pure manganese oxides in the selective catalytic reduction of nitric oxide with ammonia. *App. Catal. B., 3,* 173-189.

[28] Trevino, H., Lei, G. D. & Sachtler, W. M. H. (1995). CO Hydrogenation to Higher Oxygenates over Promoted Rhodium: Nature of the Metal-Promoter Interaction in Rhmn/NaY, *J. Catal., 154,* 245-252.

[29] De Jong, K. P., Glezer, J. H. E., Kuipers, H. P. C. E., Knoester, A. & Emeis, C.A. (1990). Highly dispersed Rh/SiO_2 and $Rh/MnO/SiO_2$ catalysts: 1. Synthesis, Characterization, and CO Hydrogenation Activity. *J. Catal., 124,* 520-529.